Microscopic distorted-wave approximation study of low-energy nucleon scattering from ^{89}Y

S. Mellema*
Department of Physics, University of Wisconsin–Madison, Madison, Wisconsin 53706

J. S. Petler† and R. W. Finlay
Department of Physics, Ohio University, Athens, Ohio 45701

F. S. Dietrich
Lawrence Livermore National Laboratory, Livermore, California 94550

J. A. Carr and F. Petrovich
Department of Physics and Supercomputer Computations Research Institute, Florida State University, Tallahassee, Florida 32306

(Received 13 March 1987)

New differential cross section data for inelastic neutron scattering to the first three excited states of ^{89}Y at $E_n = 11$ MeV are studied using a microscopic folding model and three energy- and density-dependent effective interactions. Results are also presented for the corresponding transitions in inelastic proton scattering at 14.7, 24.5, and 61.2 MeV. Transition densities were obtained from a combination of available inelastic electron-scattering data and theoretical considerations. The calculated angular distributions provide a reasonable description of the experimental data for the predominantly quadrupole ($\Delta J = 2$), $\frac{1}{2}^- \rightarrow \frac{3}{2}^-$ ($E_x = 1.509$ MeV) and $\frac{1}{2}^- \rightarrow \frac{5}{2}^-$ ($E_x = 1.745$ MeV) transitions in the target. It is shown that the neutron scattering data for these two transitions are sensitive to the shape differences in the transition densities suggested by theory and electron scattering. The theoretical results for the predominantly $\Delta J = 5$, $\frac{1}{2}^- \rightarrow \frac{9}{2}^+$ ($E_x = 0.909$ MeV) transition significantly underestimate the proton and neutron scattering cross sections at $E_p < 25$ MeV and $E_n = 11$ MeV, but provide a reasonable description of the proton scattering data for this transition at $E_p = 61.2$ MeV.

I. INTRODUCTION

Transfer reaction studies suggest that the transitions to the first three excited states of ^{89}Y at $E_x = 0.909$, 1.507, and 1.745 MeV are predominantly $2p_{1/2} \rightarrow 1g_{9/2}$ single particle, $2p_{1/2} \rightarrow 2p_{3/2}$ single hole, and $2p_{1/2} \rightarrow 1f_{5/2}$ single hole excitations, respectively.[1–3] The $2p_{1/2} \rightarrow 1g_{9/2}$ single particle transition is a well-known case of $M4$ nuclear isomerism in gamma decay[4] that proceeds primarily through $J = 5$ total angular momentum transfer in inelastic scattering.[5] The $2p_{1/2} \rightarrow 2p_{3/2}$ and $1f_{5/2}$ single hole transitions proceed mainly through $\Delta J = 2$ in inelastic scattering. These transitions are interesting because they are governed by radial transition densities with distinct shapes, owing to the different nodal structure in the radial wave functions for the $2p$ and $1f$ valence orbits. The shape differences in the transition densities are expected to give rise to corresponding differences in the shapes of the differential cross sections for the excitation of these levels by the inelastic scattering of weak to moderately absorbed probes. Theoretical estimates of the transition densities for the three transitions of interest are available from the broken-pair (BP) model of Hofstra and Allaart[6] and the core polarization studies of Petrovich *et al.*[7]

Only scant attention has been paid to the question of shape differences in the differential cross sections for the first two $\Delta J = 2$ transitions in ^{89}Y in previous low momentum-transfer electron scattering[8–10] and low energy nucleon scattering[5,11–13] studies of ^{89}Y. In some cases the scattering to the $\frac{3}{2}^-$ (1.507 MeV) and $\frac{5}{2}^-$ (1.745 MeV) levels in ^{89}Y has been described by the weak coupling model, in which the final states are interpreted as resulting from the coupling of a $2p_{1/2}$ proton to the lowest 2^+ excitation of the ^{88}Sr core. In this model the shapes of the angular distributions for scattering to the two levels are identical. A recent high momentum-transfer electron-scattering study[14,15] has yielded precise information on the proton transition densities for the first three excitations in ^{89}Y. This work strongly supports descriptions of the transitions to the second and third excited states based on the single hole picture.

Recently there has been considerable activity in describing low-energy ($\lesssim 26$ MeV) nucleon scattering data in terms of a microscopic folding model employing energy- and density-dependent effective nucleon-nucleon interactions.[16–23] In these studies, a ground-state (or transition) density is folded together with the effective interaction to yield an optical or inelastic scattering potential. Three effective interactions have been used in these investigations. These are the Brieva-Rook interaction (BR),[24] an interaction based upon the model of Jeukenne, Lejeune, and Mahaux (JLM),[25] and the interaction of Yamaguchi *et al.* (Y) (Ref. 26). In some of the calculations, the spin-dependent components of the G-matrix interaction of Bertsch *et al.* (M3Y) (Ref. 27)

have been used to supplement these interactions. All of this work has been directed toward the eventual goal of firmly establishing the combined use of electron, proton, and neutron scattering data to obtain precise information on the properties of the effective nucleon-nucleon interaction and the proton and neutron radial transition densities.[28,29]

The present work is a continuation of the studies of Refs. 16–23, with the principal aim of obtaining inelastic neutron scattering differential cross sections for the first three levels of ^{89}Y with sufficient precision to study the sensitivity of low energy neutron scattering to the detailed shapes of radial transition densities. The emphasis here is on the two $\Delta J=2$ transitions. The energy chosen (11 MeV) was low enough to allow these two transitions to be resolved. We also present results for excitation of the first three levels of ^{89}Y via inelastic proton scattering at $E_p=14.7$, 24.5, and 61.2 MeV and compare these with data from earlier experiments.[11,12,30] For excitation of the first-excited ($\frac{9}{2}^+$) state, we consider only the $\Delta J=5$ component of the transition to illustrate a problem with the energy dependence for this high-multipolarity transition.

Although a number of different model calculations have been performed in the course of this investigation, the explicit results we present for the $\Delta J=2$ transitions are based on the proton transition densities determined from electron scattering. This assumption is reasonable for neutron scattering, since low energy neutrons "see" the protons of the target nucleus about three times more strongly than the target neutrons. Therefore, the neutron differential cross sections are primarily determined by the proton transition densities.[29] Some rough estimates of the actual $\Delta J=2$ neutron transition densities based on the results of the theoretical work of Refs. 6 and 7 are considered. A definite sensitivity to the shape differences in the transition densities is observed in the present inelastic neutron scattering data. The results of the present investigation for the same two $\Delta J=2$ transitions observed in proton scattering are inconclusive with respect to these shape effects. Part of the difficulty here is associated with our loose treatment of the neutron transition densities, since incident protons in this energy region, in contrast to neutrons, couple more strongly to target neutrons than to target protons by the same factor of 3 mentioned above.[29] In a recent paper related to the present work, Kouw *et al.*[31] have clearly demonstrated that $E_p=25$–31 MeV inelastic proton scattering differential cross sections are sensitive to the differences in radial transition densities for 2^+ excitations in ^{88}Sr. The calculations for both neutron and proton excitation of the $\Delta J=5$ transition are based on the theoretical transition densities of Refs. 6 and 7, which give a good description of the (e,e′) data of Ref. 14.

II. EXPERIMENT

The present data were taken at the Ohio University beam-swinger time-of-flight (TOF) facility[32] using 11 MeV neutrons produced in a 3 cm long gas cell via the ^{2}H(d,n)^{3}He source reaction. The 100% abundant ^{89}Y scattering sample was a right circular cylinder 3 cm in diameter and 4 cm high containing 1.42 moles of ^{89}Y which was illuminated by the 0° flux from the gas cell at a distance of 19 cm. The scattered neutrons were detected by an array of seven NE213 liquid scintillator detectors at a flight path of 14 m in the TOF tunnel. Neutron/γ-ray pulse shape discrimination was used, and a dynamic (energy-dependent) bias was applied to the TOF spectra.[33] Normalization was accomplished by using a monitor detector, fixed in relation to the neutron source, and by frequent measurements in which the scattering sample was removed and the main detectors viewed the 0° flux from the gas cell. Data were taken in 5° steps from 15° to 160°, and measurements were performed both with the scattering sample present and with the sample removed in order to subtract background.

During the course of the experiment, a contaminant in the sample amounting to 0.11 moles of ^{16}O was discovered. This may be seen near channel 425 in Fig. 1, a typical background-subtracted TOF spectrum. The areas under the peaks were extracted by a peak-fitting program, and angular distributions were obtained for four states: elastic scattering from the ground state ($\frac{1}{2}^-$), and inelastic scattering from the $\frac{9}{2}^+$ ($E_x=0.909$ MeV), $\frac{3}{2}^-$ ($E_x=1.509$ MeV), and $\frac{5}{2}^-$ ($E_x=1.745$ MeV) states. Because of the ^{16}O contaminant in the sample, the inelastic angular distributions are incomplete at those angles where the contaminant TOF peak kinematically "walked through" the inelastic peak. At those forward angles where the contaminant peak could not be resolved from the elastic peak, the elastic cross sections have been corrected by subtracting the contaminant contributions estimated from an optical-model calculation.

Corrections were also made for the anisotropy of the neutron source reaction and for the energy-dependent efficiency of the neutron detectors.[33] Finally, the cross sections have been corrected for flux attenuation in the sample, for finite angular geometry, and for multiple scattering.[34] The final data contain error bars due pri-

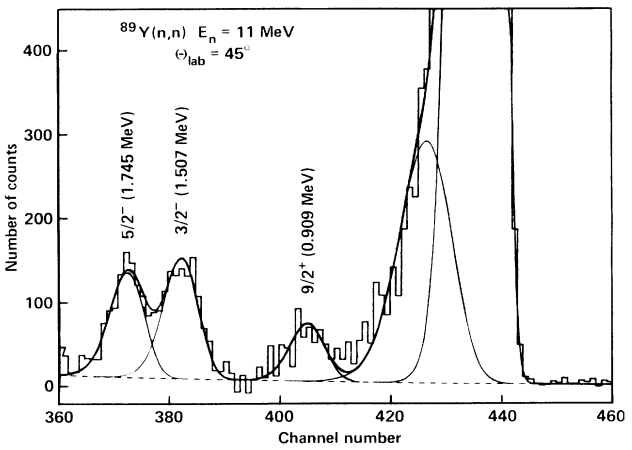

FIG. 1. Peak fit to a background-subtracted time-of-flight spectrum for 11 MeV neutron scattering from ^{89}Y. Excited states are labeled, and thin lines show the individual peak contributions to the total fit (bold line), including the ^{16}O(n,n) contaminant peak (near channel 425). The ^{89}Y elastic peak is off scale.

marily to counting statistics, but enhanced by the uncertainties in the peak-fitting procedure and in the detector-efficiency correction. The uncertainties in the elastic cross sections are 3–4 %, while those for the inelastic cross sections are typically 10–20 %. On the other hand, the overall normalization is known to $\lesssim 3\%$ due to the small uncertainties in the 0° neutron flux.

III. ELASTIC SCATTERING

The 11 MeV elastic neutron scattering data from the present experiment and the 14.7, 24.5, and 61.2 MeV elastic proton scattering data of Refs. 11, 12, and 30 were examined using the microscopic folding model based on the three density dependent effective interactions of Refs. 24–26 which were described in Sec. I. In these calculations the ground state proton charge density was taken from elastic electron scattering studies.[35] The point proton density was obtained by deconvoluting the charge densities of the constituent nucleons.[36] The ground state point neutron density was assumed to be N/Z times the point proton density. Real and imaginary central potentials and real spin-orbit potentials were calculated for all three interactions. A small spin-spin potential arising from the nonzero spin of ^{89}Y has been neglected. The spin-orbit potentials used with the BR (Ref. 24) and JLM (Ref. 25) central potentials were calculated using the Elliott form of the M3Y (Ref. 27) interaction. The Y (Ref. 26) interaction contains both central and spin-orbit components. Additional details on these calculations may be found in Refs. 16, 17, and 21.

To compare the theoretical potentials with the experimental data, we introduce normalization parameters λ_V, λ_W, and λ_{so} for the three components of the potential, and calculate the differential cross sections. In these calculations λ_{so} was fixed at the values 1.0 and 1.3, independent of energy, for the M3Y (Ref. 27) and Y (Ref. 26) spin-orbit interactions, respectively. These values were determined from previous studies of other nuclei in which both elastic differential cross section and analyzing power data were examined.[17,23] The parameters λ_V and λ_W were varied to produce a best least-squares fit to the experimental data. The values of λ_V and λ_W obtained are given in Table I, and the corresponding calculated differential cross sections are compared with the experimental data in Fig. 2. The results for 61.2-MeV elastic proton scattering were obtained primarily for the purpose of estimating the $\frac{1}{2}^- \rightarrow \frac{9}{2}^+$ ($\Delta J = 5$) inelastic cross section, and are not included in the table or the figure.

The agreement between the calculated cross sections and the experimental data is quite good. A possible exception is the neutron result obtained with the BR potential, which overestimates the differential cross section at very forward angles and gives much too deep a minimum at $\theta_{\text{c.m.}} \approx 45°$. For all three interactions, the values of λ_V are very nearly 1.0. For the JLM interaction the value of λ_W was also close to 1.0; however, the central imaginary BR potential required substantial renormalization upward, and the central imaginary Y potential a substantial renormalization downward in order to fit the data optimally. These trends are consistent with the results of previous studies for other nuclei.[17,20,21]

IV. INELASTIC SCATTERING

In our previous inelastic scattering calculations for strong collective states in even-even Fe isotopes,[19,22] we have used proton transition densities obtained from the Tassie model[37] normalized to the values of $B(EJ)$ determined in inelastic electron scattering or Coulomb excitation studies. Neutron transition densities were assumed proportional to the proton transition density. The constant of proportionality, the ratio of neutron to proton transition matrix elements M_n/M_p, was varied to fit the experimental data and thus to obtain information about isovector effects in these transitions. M_n/M_p takes on the value N/Z for the simplest hydrodynamic picture of a transition. There are significant deviations from this picture associated with shell closure.[38]

In the present work we are interested in more detailed properties of the transitions than are incorporated in the simple Tassie model.[37] Table II contains a summary of experimental and theoretical electromagnetic transition rates and multipole moments for the transitions from the ground state to the first three excited levels of ^{89}Y. We include information from γ-decay,[39,40] electron scattering,[14,15] theoretical single particle or hole estimates, and theoretical results based on a combination of the considerations of Refs. 6 and 7. In Fig. 3 we show the model-independent charge transition densities of Ref. 15 for the $\frac{1}{2}^- \rightarrow \frac{3}{2}^-$ and $\frac{5}{2}^-$ transitions which are receiving particular emphasis here. The shapes of the densities for these two states are very different, as was discussed earlier in Sec. I. The theoretical results provide a reasonable description of the measured electromagnetic transition rates. The theoretical values of M_n/M_p are in the range of approximately 0.6–1.0, which is expected for nuclei near mass 90 with a closed $N = 50$ shell.[38] There are additional shape differences between the proton and neutron transition densities predicted by the theoretical models.

Distorted-wave approximation (DWA) calculations for the natural parity ($\Delta J = 2$ and 5) contributions to the pro-

TABLE I. Normalization parameters for the real and imaginary central potentials obtained from elastic scattering analysis.

Nucleon energy (MeV)	λ_V BR	λ_V JLM	λ_V Y	λ_W BR	λ_W JLM	λ_W Y
11.0	1.02	1.00	0.96	1.31	0.95	0.58
14.7	1.05	1.02	1.00	1.39	1.06	0.66
24.5	1.06	1.00	1.00	1.64	1.02	0.70

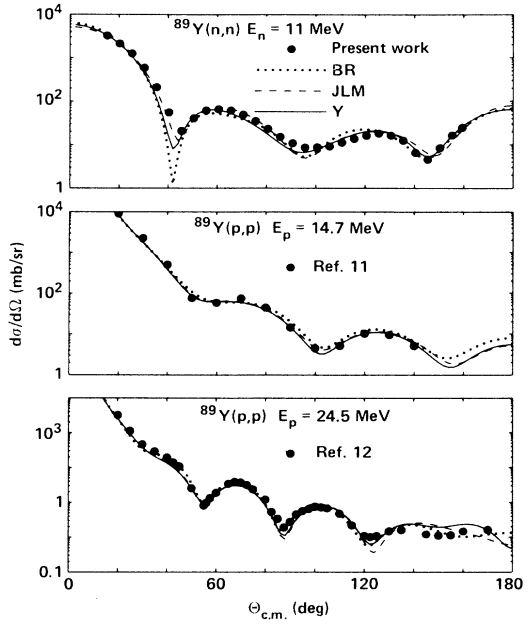

FIG. 2. Microscopic optical model calculations are compared to elastic scattering data.

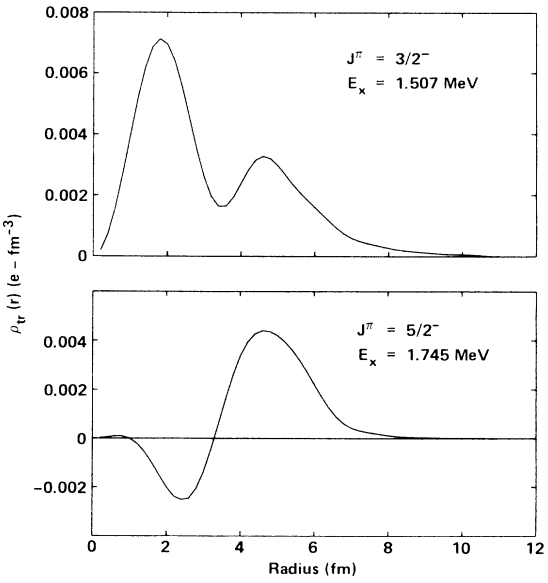

FIG. 3. Charge transition densities for the $\frac{3}{2}^-$ and $\frac{5}{2}^-$ states determined from inelastic electron scattering.

ton and neutron inelastic scattering differential cross sections for all three transitions were made, using each of the density-dependent effective interactions under consideration. Entrance- and exit-channel optical potentials and inelastic-scattering form factors were calculated in a consistent manner. The values of λ_V, λ_W, and λ_{so} obtained from the elastic scattering analysis were used throughout. The unnatural parity ($\Delta J = 1$, 3, and 4) contributions to the proton and neutron inelastic scattering cross sections were estimated in the DWA using the spin-dependent components of the M3Y interaction. The present calculations for the natural-parity contributions are essentially the same as those described in Refs. 19 and 22, except that the present calculations incorporated factors to account for the Perey effect.[41] The result of the inclusion of these factors is about a 30% decrease in the calculated cross sections, with very little change in the shape of the angular distribution. Details concerning the unnatural parity contributions to the differential cross sections may be found in Refs. 42 and 43. The Perey effect was included in these calculations as well.

Several choices for the transition densities were made in the calculations of the natural parity contributions to the differential cross sections for the three transitions of interest. One of these choices employs the theoretical neutron and proton transition densities based on the work of Refs. 6 and 7. In another prescription, the phenomeno-

TABLE II. Experimental and theoretical transition strengths for excitation of the first three excited states of ^{89}Y, together with theoretical estimates of the ratio of neutron and proton multipole matrix elements.

Transition	Moment[a]	γ decay[b]	(e,e′)[c]	SP[d]	BP + CP[e]	M_n/M_p[f]
$\frac{1}{2}^- \rightarrow \frac{3}{2}^-$	$B(M1\uparrow)$	$(8\pm5)\times10^{-3}$	7.10×10^{-3}	3.70×10^{-2}	1.69×10^{-2}	
	$B(E2\uparrow)$	$(1.04\pm0.65)\times10^{2}$	$(1.14\pm0.12)\times10^{2}$	6.23×10^{2}	1.14×10^{2}	0.76
$\frac{1}{2}^- \rightarrow \frac{5}{2}^-$	$B(E2\uparrow)$	$(2.00\pm0.15)\times10^{2}$	$(1.97\pm0.14)\times10^{2}$	6.46×10^{2}	1.97×10^{2}	1.00
	$B(M3\uparrow)$		≤ 94	4.52×10^{-1}	2.30×10^{-2}	
$\frac{1}{2}^- \rightarrow \frac{9}{2}^+$	$B(M4\uparrow)$	3.02×10^{3}	2.96×10^{3}	2.79×10^{4}	5.77×10^{3}	
	$B(E5\uparrow)$		$(5.5\pm1.6)\times10^{6}$	6.84×10^{6}	5.51×10^{6}	0.585

[a]Units for $B(EJ)$ and $B(MJ)$ are $e^2\text{fm}^{2J}$.
[b]References 9 and 40; uncertainties quoted when available.
[c]References 14 and 15; uncertainties quoted when available.
[d]Single nucleon results using harmonic oscillator radial wave functions with $b = 2.16$ fm.
[e]Single nucleon plus core polarization (Ref. 7) with spectroscopic amplitudes 0.75, 1.00, and 0.70 for $\frac{1}{2}^- \rightarrow \frac{3}{2}^-$, $\frac{5}{2}^-$, and $\frac{9}{2}^+$ transitions, respectively, as suggested by broken pair model (Ref. 6).
[f]Ratio of neutron and proton multipole matrix elements from BP + CP model calculations.

logical proton transition densities were taken from electron scattering,[14,15] together with neutron transition densities assumed to be proportional to the proton transition densities. Calculations were also made with neutron densities chosen according to the expression $\rho_n=\rho_p+\Delta\rho$, in which ρ_p is the phenomenological proton transition density, and the neutron-proton difference $\Delta\rho$ is obtained from the theoretical calculations of Refs. 6 and 7. In all calculations based on the phenomenological densities, the finite size of the constituent nucleons was deconvoluted from the transition charge densities in the same manner as described for the elastic scattering calculations. Calculations of the unnatural parity contributions to the differential cross sections were made using pure single particle or hole wave functions and the theoretical wave functions from Refs. 6 and 7. Below we present only a specific subset of the results obtained. The reason for truncating the discussion is that there are important rearrangement[44] and exchange nonlocality[45] corrections to the folding model which are currently being investigated. A more detailed description of the present calculations, with these corrections included, will be presented when these studies are complete.

A. $\frac{3}{2}^-$ ($E_x=1.509$ MeV) and $\frac{5}{2}^-$ ($E_x=1.745$ MeV) states

The $\Delta J=1$ and 3 contributions to the cross sections for the $\frac{3}{2}^-$ and $\frac{5}{2}^-$ excitations were found to be essentially negligible for both neutron and proton scattering at the energies considered here. The ratios to the $\Delta J=2$ cross sections were approximately 0.2 (0.3) and 0.05 (0.10), respectively, for the neutron (proton) scattering results. Theoretical $\Delta J=2$ cross sections for the $\frac{3}{2}^-$ and $\frac{5}{2}^-$ excitations based on the three density-dependent interactions are compared with the 11 MeV neutron data from the present work in Fig. 4. The results shown are based on the electron scattering densities and the assumption $\rho_n=(N/Z)\rho_p$. The corresponding results for 14.7 and 24.5 MeV proton scattering are shown in Figs. 5 and 6. The neutron cross sections are reduced only by about

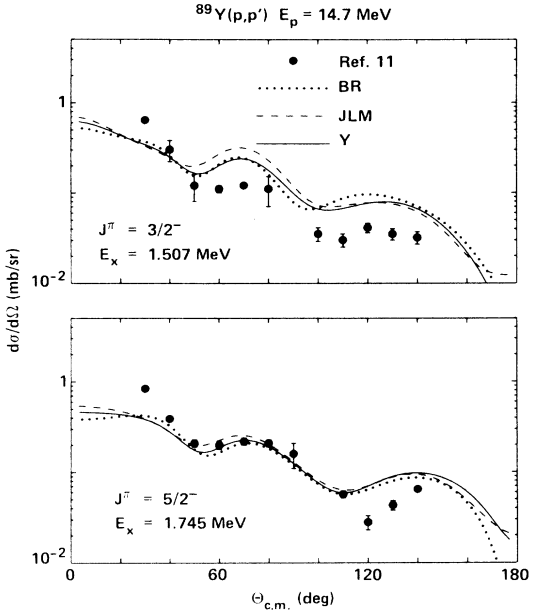

FIG. 5. Microscopic DWA calculations are compared to the proton inelastic scattering data of Ref. 11 ($E_p=14.7$ MeV) for the $\Delta J=2$ transitions.

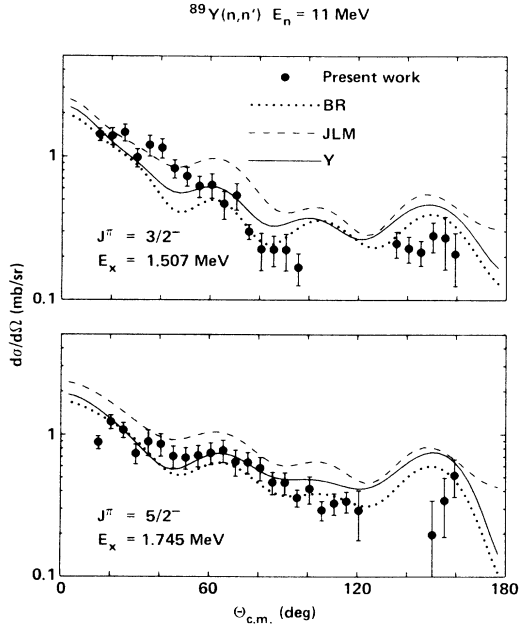

FIG. 4. Microscopic DWA calculations are compared to the present inelastic neutron scattering data ($E_n=11$ MeV) for the $\Delta J=2$ transitions.

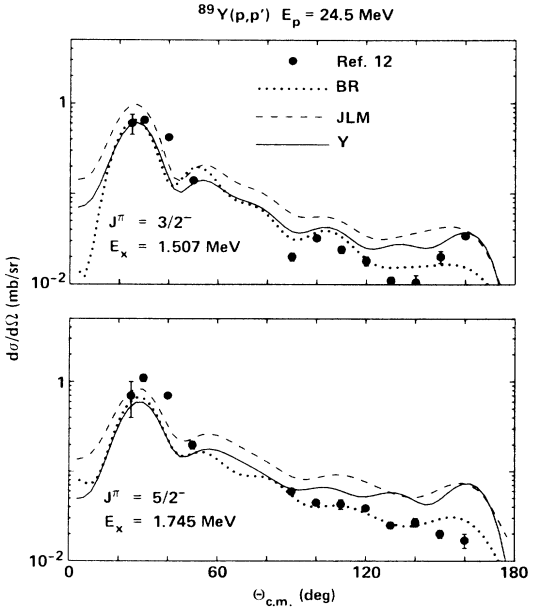

FIG. 6. Microscopic DWA calculations are compared to the proton inelastic scattering data of Ref. 12 ($E_p=24.5$ MeV for the $\Delta J=2$ transitions.

12% if $\rho_n = 0.83\rho_p$, as suggested by Table II. The same change in the neutron transition density produces about a factor of 2 change in the proton differential cross sections. This is a reflection of the dominance of the neutron-proton interaction which makes incident protons much more sensitive to the target neutrons than incident neutrons, as discussed earlier. The cross section results obtained with either the theoretical transition densities, or with the phenomenological proton densities and neutron densities not proportional to the proton densities, fall within the range of results cited above.

Overall, the agreement between the theoretical curves in Figs. 4–6 and the experimental data is not unreasonable. There are systematic differences between the three effective interactions, with the JLM model providing the largest cross sections in each case and the BR interaction producing the lowest cross sections throughout. There is a definite tendency for the theoretical cross sections to fall too slowly with increasing angle; i.e., they are either too small at forward angles or too high at backward angles, depending upon the normalization. This problem has been noted in our earlier work[19,22,28] and may be related to the neglect of rearrangement[44] and nonlocality[45] corrections in the folding model which are currently under investigation. The theoretical cross sections for the two transitions exhibit definite differences in shape, particularly at forward angles. Specifically, the theoretical cross sections for the $\frac{3}{2}^-$ excitation have a sharper forward rise than for the $\frac{5}{2}^-$. This is most evident in the 11 MeV neutron scattering results and least noticeable in the 24.5 MeV proton scattering, where the forward rise is more properly described as a forward peak.

The experimental neutron scattering cross sections in Fig. 4, which extend to 15°, show this same behavior. This is experimental evidence that quite low energy neutron scattering is sensitive to the details of the radial shapes of transition densities. To see more clearly the extent to which the neutron cross sections for the two quadrupole transitions deviate from one another and to see how well the microscopic DWA calculations reproduce this deviation, the ratio of the experimental differential cross sections for the $\frac{5}{2}^-$ and $\frac{3}{2}^-$ excitations is shown in Fig. 7 and compared with the corresponding theoretical results. The dot-dash line in Fig. 7 represents the weak coupling model which predicts that the differential cross sections should be in the ratio $(2J_a+1)/(2J_b+1)$, which is 1.5 for $J_a=\frac{5}{2}$ and $J_b=\frac{3}{2}$. This result is, of course, independent of angle. The DWA result is clearly consistent with the trend of the experimental cross section ratio, which deviates substantially from the weak-coupling limit at forward angles.

The experimental proton scattering cross sections in Figs. 5 and 6 do not clearly show the effect suggested by the theoretical calculations. The experimental proton cross section ratios, analogous to those shown in Fig. 7, do not show any clearly interpretable pattern; the points are sparse and scatter widely about the weak-coupling line. It is quite likely that the true neutron transition densities for the two quadrupole transitions are more similar than allowed by the proportionality of ρ_p and ρ_n that is assumed in the calculation displayed in Figs. 5 and 6. The theoretical cross sections obtained with neutron transition densities based on the theoretical wave functions of Refs. 6 and 7 (not shown) do, in fact, bear this out. The recent work of Kouw *et al.*[31] contains an example of two transitions in ^{88}Sr that are governed by quite different neutron transition densities which lead to clear differences in the shape of low energy proton scattering angular distributions.

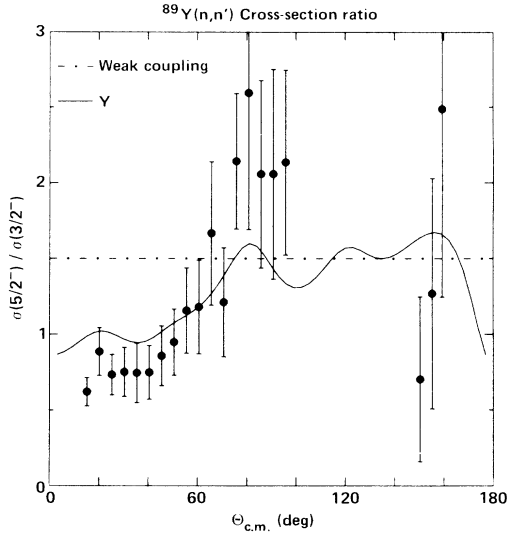

FIG. 7. The ratios of the $\frac{5}{2}^-$ and $\frac{3}{2}^-$ experimental cross sections for neutron scattering at 11 MeV are compared with the calculations of the weak-coupling model (dot-dashed line) and the microscopic model using the Yamaguchi interaction (solid line).

B. $\frac{9}{2}^+$ ($E_x = 0.909$ MeV) state

Theoretical results for the excitation of the $\frac{9}{2}^+$ ($E_x = 0.909$ MeV) level in ^{89}Y for 11 MeV neutrons and 14.7, 24.5, and 61.2 MeV protons are compared with the available experimental data in Fig. 8. We show only the JLM results for the natural parity ($\Delta J = 5$) contribution. The theoretical transition densities based on the work of Refs. 6 and 7 have been used in obtaining the particular results shown. The $\Delta J = 4$ unnatural parity contribution is not completely negligible for this transition. Although it is not shown, the $\Delta J = 4$ contribution is most important in increasing the width of the main peak of the angular distribution for the excitation of this level by 61.2 MeV protons. This point has been discussed in the literature previously;[7,46] see, for example, Fig. 14 of Ref. 7.

There is reasonable agreement between the theoretical results and the experimental proton scattering data for the $\frac{9}{2}^+$ excitation at $E_p = 61.2$ MeV, but the theoretical cross sections significantly underestimate the experimental proton and neutron scattering cross sections at the lower energies. The discrepancy between theory and experiment increases with decreasing energy. Preliminary plane-wave calculations for the $\frac{9}{2}^+$ transition in ^{89}Y, with the ex-

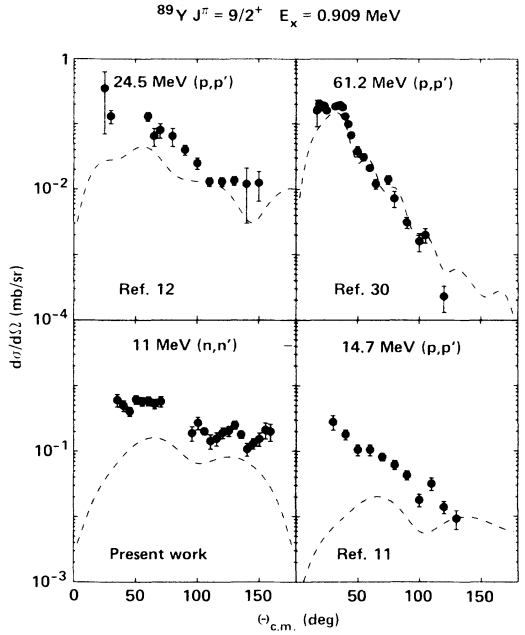

FIG. 8. Microscopic DWA calculations using the JLM interaction are compared with data from the present work and Refs. 11, 12, and 30 for the $\Delta J = 5$ transition to the $\frac{9}{2}^+$ ($E_x = 0.909$ MeV) state.

change nonlocality treated exactly via the techniques of Ref. 45, suggest that there are important corrections to the $\Delta J = 5$ cross section at low momentum transfer which are not included in the simplest exchange approximations employed in the present form of the folding model.[19,22,28] These results are expected to apply quite generally to high spin natural parity transitions at low momentum transfer. The outstanding questions concern the manner in which these low momentum transfer effects are translated into the differential cross sections when distortion is important. It is expected that the distortion effects at low energy magnify the importance of the low momentum transfer components of the transition amplitude; therefore, a possible explanation of the difficulty with the energy dependence of the theoretical cross sections shown in Fig. 8 is at hand. Investigations of these distortion effects are currently in progress.

V. CONCLUSIONS

New differential cross section data for the excitation of the first three levels in ^{89}Y by incident neutrons at $E_n = 11$ MeV have been presented. Theoretical folding-model calculations based on contemporary energy- and density-dependent effective interactions have been compared with the new neutron-scattering data and with relevant proton-scattering data. The transition densities used in these calculations have been taken from previous electron scattering studies and available theoretical calculations. It is shown that the neutron scattering cross sections for the two predominantly quadrupole transitions considered are sensitive to the shape differences in the proton transition densities suggested by electron scattering and theory, even though the incident energy is low. Corresponding proton scattering data for these transitions at $E_p \leq 24.5$ MeV show no clear signature of shape differences, which probably indicates that the differences in the shapes of the neutron transition densities are less pronounced than for the proton transition densities. However, more detailed proton scattering data would provide a basis for strengthening this last remark.

Although the theoretical results provide a reasonable qualitative description of the data, there are definite discrepancies between theory and experiment. These are in the fore-aft behavior of the differential cross sections for the quadrupole excitations and the energy dependence of the differential cross sections for the $\frac{1}{2}^- \rightarrow \frac{9}{2}^+$ transition. These discrepancies are consistent with problems noted in earlier studies.[19,22,28] It is suggested that rearrangement[44] and exchange[45] corrections to the folding model might account for the discrepancies. These are currently under investigation. If a successful conclusion to these studies is obtained, the combined use of electron, neutron, and proton scattering data to provide detailed information on the properties of effective interactions and target proton and neutron transition densities will become an important spectroscopic tool.

ACKNOWLEDGMENTS

We are indebted to Prof. J. Heisenberg for providing us with the electron-scattering results that were used for the phenomenological proton transition densities. This work was supported by the U.S. National Science Foundation under Grants No. PHY-8414810, PHY-8108456, and PHY-8122131, and by the U.S. Department of Energy under Contract No. W-7405-ENG-48 and cooperative agreement No. DE-FC05-85ER250000. S.M., J.A.C., and F.P. wish to thank the Lawrence Livermore National Laboratory for hospitality extended to them while a part of this work was performed.

*Present address: Physics Department, Gustavus Adolphus College, St. Peter, MN 56082.

†Present address: Exploration Division, British Petroleum Research Centre, Sunbury-on-Thames, Middlesex, United Kingdom.

[1]C. D. Kavaloski, J. S. Lilley, D. C. Shreve, and N. Stein, Phys. Rev. **161**, 1107 (1967).

[2]G. Vourvopoulos and J. D. Fox, Phys. Lett. **25B**, 543 (1967); Phys. Rev. **177**, B155 (1969).

[3]G. Vourvopoulos, R. Shoup, and R. A. Brown, Nucl. Phys. **A174**, 581 (1971).

[4]M. Goldhaber and A. W. Sunyar, Phys. Rev. **83**, 906 (1951).

[5]M. M. Stautberg, J. J. Kraushaar, and B. W. Ridley, Phys. Rev. **157**, 977 (1967).
[6]P. Hofstra and K. Allaart, Z. Phys. A **292**, 159 (1979).
[7]F. Petrovich, H. McManus, J. Borysowicz, and G. R. Hammerstein, Phys. Rev. C **16**, 839 (1977).
[8]G. A. Peterson and J. Alster, Phys. Rev. **166**, 1136 (1968).
[9]G. P. Fivozinsky, S. Penner, J. W. Lightbody, and D. Blum, Phys. Rev. C **9**, 1533 (1974).
[10]R. P. Singhal *et al.*, J. Phys. G **5**, 558 (1975).
[11]Y. Awaya, J. Phys. Soc. Jpn. **23**, 673 (1967).
[12]W. Benenson, S. M. Austin, and R. A. Paddock, Phys. Rev. **176**, 1268 (1968).
[13]Y. Yiming *et al.*, Nucl. Phys. **A390**, 449 (1982).
[14]O. Schwentker *et al.*, Phys. Lett **112B**, 40 (1982).
[15]O. Schwentker *et al.*, Phys. Rev. Lett. **50**, 15 (1983).
[16]F. S. Dietrich, R. W. Finlay, S. Mellema, G. Randers-Pehrson, and F. Petrovich, Phys. Rev. Lett. **51**, 1629 (1983).
[17]S. Mellema, R. W. Finlay, F. S. Dietrich, and F. Petrovich, Phys. Rev. C **28**, 2267 (1983).
[18]Ch. Lagrange and J. C. Brient, J. Phys. (Paris) **44**, 27 (1983).
[19]S. Mellema, R. W. Finlay, F. S. Dietrich, and F. Petrovich, Phys. Rev. C **29**, 2385 (1984).
[20]L. F. Hansen, F. S. Dietrich, B. A. Pohl, C. H. Poppe, and C. Wong, Phys. Rev. C **31**, 111 (1985).
[21]J. S. Petler, M. S. Islam, R. W. Finlay, and F. S. Dietrich, Phys. Rev. C **32**, 673 (1985).
[22]S. Mellema, R. W. Finlay, and F. S. Dietrich, Phys. Rev. C **33**, 481 (1986).
[23]N. L. Back *et al.*, Bull. Am. Phys. Soc. **29**, 640 (1984); **30**, 702 (1985).
[24]F. A. Brieva and J. R. Rook, Nucl. Phys. **A291**, 299 (1977); **A291**, 317 (1977).
[25]J. P. Jeukenne, A. Lejeune, and C. Mahaux, Phys. Rev. C **16**, 80 (1977).
[26]N. Yamaguchi, S. Nagata, and T. Matsuda, Prog. Theor. Phys. (Jpn.) **70**, 459 (1983).
[27]G. Bertsch, J. Borysowicz, H. McManus, and W. G. Love, Nucl. Phys. **A284**, 399 (1977).
[28]F. S. Dietrich and F. Petrovich, in *Neutron-Nucleus Collisions—A Probe of Nuclear Structure (Burr Oak),* Proceedings of the Conference on Neutron-Nucleus Collisions—A Probe of Nuclear Structure, AIP Conf. Proc. No. 124, edited by J. Rapaport, R. W. Finlay, S. M. Grimes, and F. S. Dietrich (AIP, New York, 1985), p. 90.
[29]J. A. Carr, F. Petrovich, and J. Kelly, see Ref. 28, p. 230.
[30]A. Scott, M. L. Whiten, and J. B. Ball, Phys. Lett. **25B**, 463 (1967); C. B. Fulmer, J. B. Ball, A. Scott, and M. L. Whiten, Phys. Rev. **181**, 1565 (1969).
[31]L. R. Kouw, H. P. Blok, M. Pignanelli, R. de Leo, and M. N. Harakeh, Phys. Lett. **174B**, 137 (1986).
[32]R. W. Finlay *et al.*, Nucl. Instrum. Methods **198**, 197 (1982).
[33]S. Mellema and J. S. Petler, Nucl. Instrum. Methods **A242**, 265 (1986).
[34]W. E. Kinney, Oak Ridge National Laboratory Report ORNL-TM-2052, 1968.
[35]C. W. DeJager, H. DeVries, and C. DeVries, At. Data Nucl. Data Tables **14**, 79 (1974).
[36]G. R. Satchler and W. G. Love, Phys. Rep. **55**, 197 (1979).
[37]L. J. Tassie, Aust. J. Phys. **9**, 407 (1956).
[38]V. A. Madsen and V. R. Brown, Phys. Rev. Lett. **52**, 176 (1984).
[39]H. P. Yule, Nucl. Phys. **A94**, 442 (1967).
[40]D. C. Kocher, Nucl. Data Sheets **16**, 445 (1975).
[41]F. G. Perey and D. S. Saxon, Phys. Lett. **10**, 107 (1964).
[42]F. Petrovich, J. A. Carr, R. J. Philpott, and H. McManus, in *Proceedings of the International Symposium on Electromagnetic Properties of Atomic Nuclei,* edited by H. Horie and H. Ohnuma (Tokyo Institute of Technology, Tokyo, 1984), p. 312.
[43]F. Petrovich, J. A. Carr, and H. McManus, Annu. Rev. Nucl. Part. Sci. **36**, 29 (1986).
[44]T. Cheon, K. Takayanagi, K. Yazaki, Nucl. Phys. **A437**, 301 (1985); **A445**, 227 (1985).
[45]F. Petrovich, J. A. Carr, R. J. Philpott, and A. W. Carpenter, submitted to Phys. Rev. Lett.
[46]M. L. Whiten, A. Scott, and G. R. Satchler, Nucl. Phys. **A181**, 417 (1972).